Radioimmunoimaging of Lung Vessels: An Approach Using Indium-111-Labeled Monoclonal Antibody to Angiotensin-Converting Enzyme

Sergei M. Danilov, Andrei V. Martynov, Alexander L. Klibanov, Mikhail A. Slinkin, Ivan Yu. Sakharov, Alexandr G. Malov, Vladimir B. Sergienko, Alexandr Yu. Vedernikov, Vladimir R. Muzykantov, and Vladimir P. Torchilin

Institute of Experimental Cardiology, Institute of Clinical Cardiology, USSR Cardiology Research Center, Moscow, USSR, Laboratory of Biologically Active Substances from Hydrobionts, Ministry of Health, Moscow, USSR

A murine monoclonal antibody against human angiotensin-converting enzyme was radiolabeled with ^{111}In via diethylenetriaminepentaacetic acid without substantial loss of antigen-binding capacity. This monoclonal antibody designated 9B9 cross-reacted with rat and monkey angiotensin-converting enzyme. Indium-111-labeled 9B9 selectively accumulated 10–20 times greater in the lung than in blood or other organs following intravenous administration in rats. Kinetics of lung accumulation and blood clearance were studied for ^{111}In-9B9-antibody and compared to that of ^{125}I-labeled 9B9 in rat. Highly specific accumulation of ^{111}In-9B9-antibody in the lung of Macaca Rhesus monkeys after intravenous injection was monitored by gamma-imaging. Images of ^{111}In-labeled antibody 9B9 biodistribution in monkey lung noticeably differ from the images of biodistribution of ^{99m}Tc-labeled albumin microspheres. This difference may provide information concerning the state of the endothelium of lung capillaries, which is different from the blood flow characteristics determined with routine microsphere technique.

J Nucl Med 30:1686–1692, 1989

Mouse monoclonal antibody (MoAb) to human angiotensin-converting enzyme (ACE), designated 9B9 cross-reacted with rat and monkey ACE. Following i.v. injection, ^{125}I-9B9 accumulated in the rat lung 10 to 20 times greater than in other organs including blood (*1*). Preferential accumulation of MoAb 9B9 in the lung can be attributed to a high concentration of pulmonary ACE (*2,3*). It is not clear whether the high concentration of pulmonary ACE is due only to a large surface of pulmonary vasculature (*4*) or is associated with a high ACE density on lung capillary endothelium.

It was shown earlier immunohistochemically with polyclonal anti-ACE antibodies, that ACE in the normal lung is also expressed on the luminal surface of the blood vessel endothelium plasma membranes (both for capillaries and large vessels) also (*5,6*). We have shown immunohistochemically that 9B9 antibodies bind to the endothelium of the capillaries and large vessels of the normal human lung tissue specimens as well (*7*). In connection with the fact that 9B9 accumulate in the rat lung, this led us to study the possibility of the use of radiolabeled 9B9 antibody usefulness for the gamma-scintigraphic visualization of lung vessels.

We can speculate on the hypothetical areas of potential clinical utility of these radiolabeled antibodies. First, we can expect that antibody lung accumulation will be lower in pathologic conditions resulting in massive damage of lung vessels and capillaries. Second, we can not exclude that 9B9 lung accumulation will be increased in case of sarcoidosis, a disease characterized with high level of ACE synthesis in lung, mainly in granuloma cells, not in endothelium (*8*). The possibility exists that the lung accumulation pattern of 9B9 anti-

Received Oct. 21, 1988; revision accepted June 21, 1989.

For reprints contact: S. M. Danilov, PhD, Institute of Experimental Cardiology, USSR Cardiology Research Centre, 3rd Cherepkovskaya ST 5A Bldg. 7, Moscow 121552 USSR

bodies will be altered in cases of primary and metastatic lung tumors. Finally, one could expect that 9B9 will be selectively accumulated in hemangioma areas.

In the present study we analysed the kinetics of distribution, lung accumulation and blood clearance of ^{111}In-labeled 9B9 as compared to ^{125}I-labeled 9B9. Furthermore, gamma-imaging with ^{111}In-labeled 9B9 was performed to determine the potential of 9B9 as a diagnostic tool for lung vessel visualization.

MATERIALS AND METHODS

Antibody Preparation

MoAb 9B9 (IgG_1) was obtained by standard hybridoma method using angiotensin-converting enzyme from human lung as the antigen (*9*). This MoAb interacts with both soluble and immobilized ACE, not inhibiting its enzymatic activity, i.e., the catalytic site of the enzyme is not involved in the 9B9 antibody binding.

MoAb 9B9 and control normal mouse IgG were isolated by DEAE-cellulose ion exchange chromatography from ammonium sulfate precipitate of ascites fluid and mouse serum, respectively. Purity of MoAb 9B9, as estimated by sodium dodecyl sulfate polyacrylamide gel electrophoresis, was >90%. Normal mouse serum polyclonal IgG was used in control experiments.

Radioiodination

Radiolabeling of antibodies with ^{125}I was performed by the Iodogen method (*10*). Briefly, 500 μg of antibodies was incubated with 0.5 mCi of $Na^{125}I$ and 2 μg of Iodogen. Each reaction was performed at 0°C for 20 min and then the protein was separated from unbound ^{125}I by Sephadex G-25 column chromatography. The specific radioactivity of the radioiodinated antibody was estimated to be between 0.1–0.2 mCi/mg.

Indium-111-Labeling

Antibodies were labeled with ^{111}In using diethylenetriaminepentaacetic acid (DTPA) as a bifunctional chelating agent (*11*). Briefly, a tenfold molar excess of cyclic DTPA anhydride dissolved in dry dimethylsulfoxide to the concentration of 0.7 mg/ml was added to 1 mg of protein (1 mg/ml in 0.1*M* $NaHCO_3$). After removing unconjugated DTPA by Sephadex G-50 column chromatography 200 μg of DTPA-conjugated protein was mixed with 1 mCi of ^{111}In (v/o Izotop, USSR) (carrier-free) added as the solution in 0.1*M* citrate, pH 6.0. Unbound ^{111}In was removed on Chelex-100 minicolumns. At least 70% of added ^{111}In was recovered in the protein fraction. The conjugation and labeling protocol yielded antibodies with 0.5 to 1.0 DTPA molecules per protein molecule and with a specific radioactivity 2–5 mCi/mg.

Immunoreactivity

Retention of antigen-binding capacity of radiolabeled MoAb 9B9 was tested by the inhibition of radioimmunoadsorbtion (*12*) with nonlabeled MoAb 9B9. ACE isolated from the human lung (*13*) was covalently immobilized on BrCN-activated Sepharose 4B (Pharmacia Fine Chemicals, Uppsala, Sweden) according to manufacturer's recommendation. ACE-Sepharose (250 μl Sepharose 4B containing 5 μg immobilized ACE) or "empty" Sepharose 4B (as a control) were incubated with PBS containing 0.2% BSA with and without 100 μg MoAb 9B9 for 1 hr at room temperature. After triple washing with PBS-BSA by centrifugation ^{111}In-labeled MoAb 9B9 (100×10^3 cpm, 0.05 μg) was incubated with pretreated immunoadsorbent for 1 hr. The unbound radioactivity was washed out with PBS-BSA by multiple centrifugation. The immunoadsorbent-bound radioactivity was counted in a gamma counter (LKB Compugamma, Wallac OY, Finland).

In Vivo Administration of Radiolabeled Antibodies

For tissue distribution studies 5 to 10 μg of labeled MoAb 9B9 or control IgG in PBS-BSA were injected into Wistar rats (weighing 150–250 g) via the tail vein. The rats were killed at indicated time intervals. Blood samples were collected in heparinized test tubes and selected internal organs were removed, washed, weighted, and their radioactivity measured in a gamma counter. In separate experiments, to study the specificity of labeled-9B9 accumulation in the lung, 10 μg ^{125}I- or ^{111}In-labeled MoAb 9B9 were diluted with different amounts of unlabeled ("cold") MoAb 9B9 prior to injection into the tail vein. The rats were killed 4 hr after the injection and the radioactivity was measured as described above. Biodistribution data were represented as a percentage of the injected dose per gram of tissue. Localization ratios of organ radioactivity (cpm/g) to the blood radioactivity (cpm/g) were also determined. The specificity of antibody localization in a given tissue was also expressed as the immunospecificity, which is defined as the antibody concentration in the tissue divided by the nonspecific immunoglobulin concentration in this tissue (*14*).

Gamma Imaging

Gamma imaging studies were performed in Macaca Rhesus monkeys (weighing 8–10 kg) following i.v. injection of 0.5 mCi (200 μg) of ^{111}In-labeled antibodies or with technetium-99- (^{99m}Tc) labeled (0.5 mCi) albumin microspheres via the femoral vein. Animals were imaged with a large field-of-view gamma camera (Gamma-Tome-2, "CGR", France). Imaging was performed with the animals placed in the prone position on the face of the high sensitivity parallel hole collimator (400 mm in diameter).

The images were digitized to the 128 × 128 matrix and computer-processed. Regions of interest (chest) were manually drawn and the data expressed as number of counts per pixel. Ketamine (5 mg/kg) given by intramuscular injection prior to each imaging procedure ensured adequate anesthesia. Typically, 100,000–200,000 counts were acquired for each view using a 20% window centered over 174 keV and 247 keV gamma ray peaks of ^{111}In and 140 keV peak energy of ^{99m}Tc.

RESULTS

Pharmacokinetics of MoAb 9B9 in Rats

Data presented in Table I clearly show that ^{111}In MoAb 9B9 binds to the ACE-Sepharose with high specificity as compared with control Sepharose 4B. The binding is inhibited by the excess of unlabeled antibody; this confirms that ^{111}In-labeled MoAb 9B9 retains its antigen-binding properties.

Upon i.v. injection of the radiolabeled antibody preparation the radioactivity was selectively accumulated in

TABLE 1
Inhibition of ^{111}In-labeled MoAb 9B9 Adsorption on ACE-Sepharose by Unlabeled MoAb 9B9

Antibody	Bound radioactivity, cpm*	
	ACE-Sepharose 4B	"empty" Sepharose 4B
^{111}In-9B9	6149 ± 249	1092 ± 72
^{111}In-9B9 plus 100 μg unlabeled 9B9	1170 ± 80	1120 ± 100

* Mean of four experiments ± s.e.

the lung. The localization ratio increased up to 12 in 3 hr postinjection (Fig. 1).

Immunospecificity as defined in the Method section for the lung reached a high value of 28 3 hr after injection of MoAb 9B9. For other tissues studied, the immunospecificity value is close to 1.

The specificity of [^{111}In]MoAb accumulation in rat lung is confirmed by the dose dependence curves. The dramatic decrease of lung radioactivity when unlabeled MoAb 9B9 was coinjected with ^{111}In-9B9 showed that ^{111}In accumulation in lung is saturable (Fig. 2). The comparison of the inhibition curves for ^{111}In-DTPA-MoAb 9B9 and ^{125}I-MoAb 9B9 shows that the labeling with ^{111}In via DTPA residues may cause greater antibody inactivation, than the labeling with ^{125}I.

The kinetics of the lung accumulation and blood clearance of ^{111}In-MoAb 9B9 is presented in Figure 3. The maximal antibody concentration in the target area is reached within 10–30 min postinjection of the radiotracer. There was a subsequent decrease of activity by two-fold in 4.5 hr. However, target-to-blood radioactivity ratio remained constant with significant increases after 24 hr.

In general, rat lung uptake of ^{111}In-MoAb-9B9 is similar to that of ^{125}I-MoAb 9B9 which is described earlier (*1*). However, there are differences in the kinetics of radiolabel accumulation. Table 2 shows that the lung localization ratio of ^{125}I-MoAb 9B9 increased from 5 to 16 during the first 24 hr after injection, whereas ^{111}In-MoAb 9B9 value stayed unchanged for several hours. This difference may be attributed to the prolonged retention of ^{125}I-MoAb 9B9 in the lung which does not appear to occur with ^{111}In-MoAb 9B9.

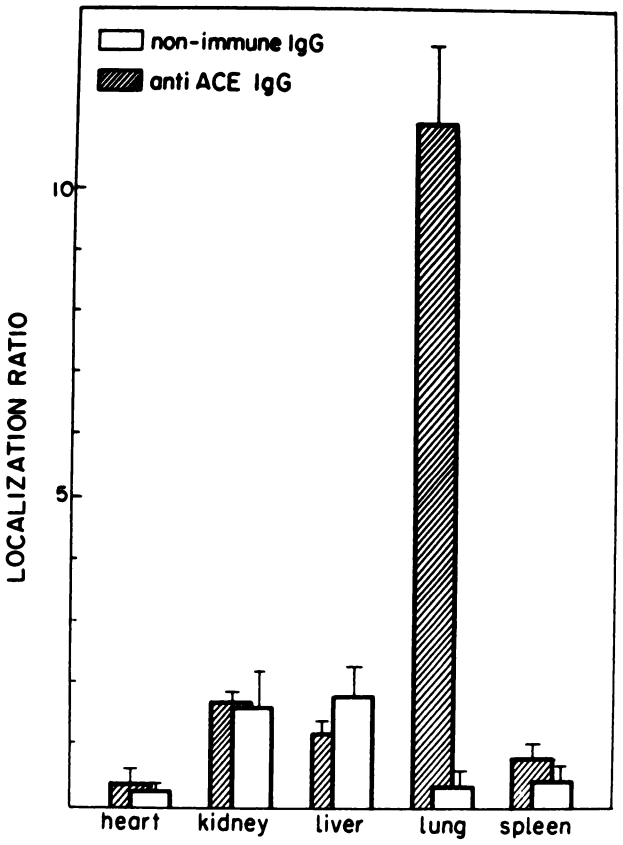

FIGURE 1
Tissue distribution of ^{111}In-labeled MoAb 9B9 in rats. Radioactivity in tissues was determined as described in the "Materials and Methods" section, 3 hr after i.v. injection of 10 μg ^{111}In-labeled MoAb 9B9 (close bars) or IgG (open bars). Distribution data were represented as a localization ratio, i.e., ratio of radioactivity of organ (cpm/g) to the radioactivity of blood (cpm/g). Mean ± s.e.m. for four to five animals.

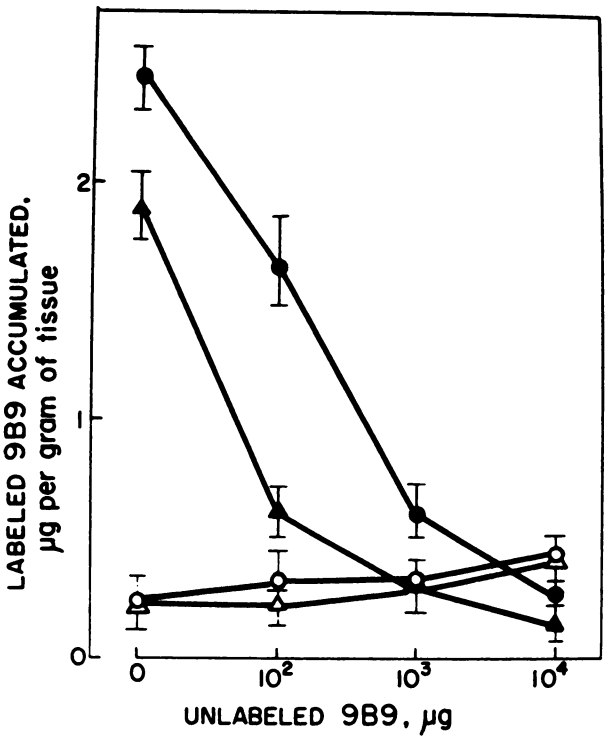

FIGURE 2
Inhibition of radiolabeled MoAb 9B9 accumulation in the rat lungs by unlabeled MoAb 9B9. Radioactivity in the rat lungs and blood was determined 3 hr after co-injection of 10 μg of radiolabeled MoAb 9B9 with indicated excess of unlabeled MoAb 9B9. Data are represented as μg of MoAb 9B9 per g of tissue. Mean ± s.e.m. for four animals. (▲) ^{111}In-labeled 9B9; (●) ^{125}I-labeled 9B9; open symbols—blood, close symbols—lung.

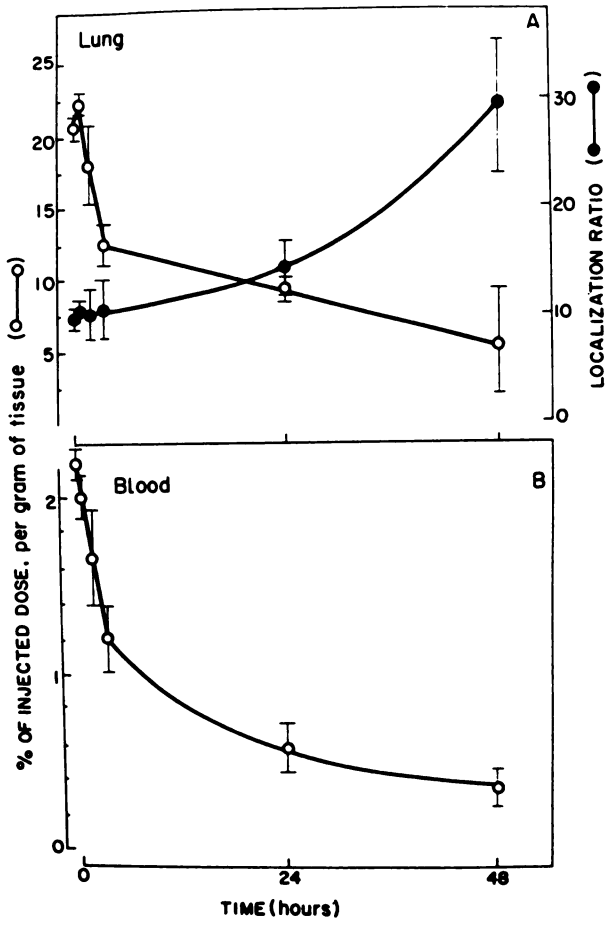

FIGURE 3
Kinetics of lung accumulation (A) and blood clearance (B) of ^{111}In-labeled 9B9. Radioactivity in the rat lung and blood was determined at indicated time intervals after i.v. injection of 10 μg ^{111}In-labeled MoAb 9B9. Distribution data were represented as a percentage (mean ± s.e.m., n = 4) of the injected dose per gramm of tissue (O). Localization ratio (mean ± s.e.m.) was also determined (●).

This difference in the ^{111}In- and ^{125}I-antibodies behaviour in vivo is also supported by the ^{125}I/^{111}In ratio values for the lung and blood samples (Table 2).

Imaging of ^{111}In-labeled MoAb 9B9 in Monkeys

The pronounced difference in the biodistribution and lung accumulation of ^{111}In-MoAb 9B9 versus ^{111}In-nonspecific mouse IgG (control) was also seen on rat gamma images (data not shown). Due to the small size of rats for imaging of lung fields and MoAb 9B9 cross-reactivity not only with rat ACE, but also with monkey ACE, ^{111}In-MoAb 9B9 lung localization was studied in Macaca Rhesus monkeys. Biodistribution and visualization studies were performed by means of gamma scintigraphy.

Figure 4 represents the gamma images of monkeys performed 1 hr after i.v. injection of ^{111}In-MoAb 9B9 or ^{111}In-nonspecific mouse IgG. The monkey lung preferentially accumulated ^{111}In attached to MoAb 9B9 similar to this antibody accumulation in rat lung. Quantitative biodistribution data for monkeys were provided not from tissue samples, as in rats, but from the image characteristics. Average count density over the lung area for the ^{111}In-MoAb 9B9 images was 164 counts per pixel and 88 counts per pixel for ^{111}In-labeled control nonimmune mouse IgG.

Figure 5 shows the images of ^{111}In-MoAb 9B9 distribution in monkeys at different time points. The lung uptake of the radiolabeled preparation was maximal for the first 24 hr with subsequent decrease with time. Therefore the images of the lung showed poor uptake in the 48 hr postinjection images. Average count density over the lung area for the ^{111}In-MoAb 9B9 images 3, 24, 48, 96 hr after injection was 160, 135, 97, and 52 counts per pixel, respectively.

Lung images obtained with ^{111}In-MoAb 9B9 were compared with those of ^{99m}Tc-albumin microspheres, which are routinely used for lung studies. Gamma tomographic serial sections presented in Figure 6 clearly showed differences in ^{111}In and ^{99m}Tc lung accumulation.

DISCUSSION

The potential of imaging lung vessels was shown by the demonstration that ^{125}I-anti-ACE MoAb 9B9 accumulated selectively in the rat lung (*1*) and that ACE localized on the membranes of blood vessels endothelium, including the lung endothelium (*5–7*). These experimental studies indicate the possibility of future clinical noninvasive application.

MoAb 9B9 was labeled with ^{111}In via DTPA, a bifunctional chelating agent. Radiolabeled antibody retained its antigen-binding capacity (Table 1). Meanwhile, biodistribution data presented on Figure 2 show that the labeling with ^{111}In inactivates MoAb 9B9 to a greater extent than the routine radioiodination procedure. The saturation of 9B9 antibody binding sites in the rat lung occurs after the injection of ~1 mg MoAb 9B9 per Wistar rat weighing 200 g. In this case antibody concentration in the lung and in the blood is similar, i.e. there is no selective lung uptake.

Due to the high specific radioactivity of the MoAb labeled with ^{111}In, (2–5 mCi/mg protein), it was sufficient to inject 10–50 μg of ^{111}In-MoAb 9B9 per rat for the imaging studies. This dose of 9B9 is at a subsaturation concentration (compare with Fig. 2) and therefore allows a high degree of lung uptake. In our experiments, specificity which was expressed as the target-to-blood localization ratio was 10 to 12 for the first hour which increased to 20–30 or higher for the period of several days (see Fig. 1, Table 2). These values are much higher than the minimal target-to-background ratio (2:1 to 5:1) which is necessary for the successful

TABLE 2
Accumulation Kinetics of ^{111}In- and ^{125}I-labeled MoAb 9B9 in rat lung and blood. (mean ± s.e.m., n = 4)

Time	10 min	30 min	90 min	270 min	24 hr	48 hr
^{125}I-labeled 9B9						
% dose per g of lung tissue	23.8 ± 0.3	25.9 ± 0.7	29.8 ± 4.0	25.0 ± 4.0	16.7 ± 2.3	9.5 ± 2.9
% dose per g of blood	4.7 ± 1.2	2.9 ± 0.6	2.9 ± 0.1	1.9 ± 0.3	1.0 ± 0.1	0.7 ± 0.1
Local. ratio	5.2 ± 1.2	9.2 ± 1.9	10.1 ± 2.3	13.4 ± 0.3	16.2 ± 1.2	13.3 ± 3.0
^{111}In-labeled 9B9						
% dose per g of lung tissue	21.7 ± 0.9	22.8 ± 0.9	18.5 ± 4.6	12.6 ± 4.0	9.2 ± 0.1	5.3 ± 3.8
% dose per g of blood	2.2 ± 0.1	2.0 ± 0.2	1.7 ± 0.4	1.1 ± 0.2	0.9 ± 0.1	0.2 ± 0.1
Local. ratio	9.9 ± 0.2	11.4 ± 1.3	10.9 ± 0.2	11.4 ± 1.9	16.2 ± 3.6	28.1 ± 5.1
% dose per g, ^{125}I/^{111}In ratio						
Lung	1.1 ± 0.1	1.1 ± 0.1	1.6 ± 0.5	2.0 ± 0.7	1.8 ± 0.3	1.8 ± 1.4
Blood	2.2 ± 0.6	1.5 ± 0.3	1.7 ± 0.4	1.7 ± 0.4	1.7 ± 0.4	3.9 ± 2.2

imaging of certain targets from theoretic considerations for detection of deep and small lesions (*15*). The immunospecificity which is defined as the localization ratio for the specific antibody accumulation in the given tissue divided by the localization ratio for the nonspecific immunoglobulin of the same isotype in the said tissue is another important measure of specific antibody accumulation (*14*). Immunospecificity of ^{111}In-MoAb 9B9 uptake in rat lung was very high (*28*) 3 hr after antibody injection (see Fig. 1).

It should be possible to increase the specificity of MoAb 9B9 accumulation in the lung. This can be achieved by utilization of F(ab)$_2$ or F(ab)-fragments of MoAb instead of whole IgG molecules. This approach for tumor-specific antigens was successfully applied by Sakahara et al. (*16*) and Wahl et al. (*17*). However, in certain cases, application of antibody fragments may not improve imaging due to high radioactivity accumulation in the liver and kidney (*16*). Nevertheless, the preparation of F(ab')$_2$ and F(ab)-fragments of MoAb 9B9, their radiolabeling and biodistribution studies are now in progress in our laboratory.

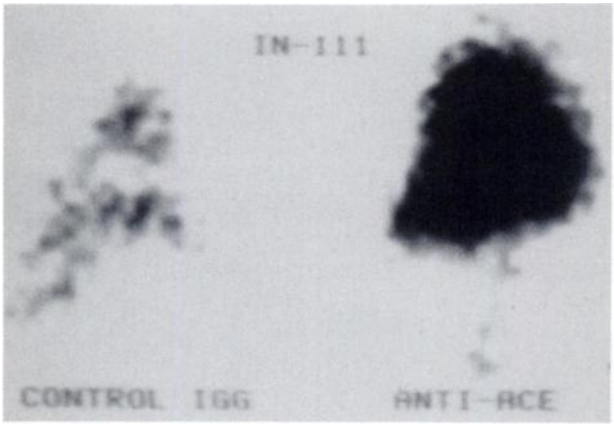

FIGURE 4
Anterior thoraco-abdominal gamma scintigrams showing the localization of ^{111}In-labeled MoAb 9B9 (right) and normal mouse IgG (left) 1 hr after i.v. administration of the radiolabeled antibodies (200 μg; 0.5 mCi) in monkeys. Background radioactivity was subtracted from each image.

Recently we demonstrated that radiolabeled 9B9 antibody may be cleared from the circulation by various approaches (*18*), including (a) application of the second antibody to rapidly decrease the blood activity and (b) by chemical modification of MoAb 9B9 with lactose or (c) injection of excessive amount of avidin in the blood with circulating biotinylated MoAb 9B9. All the above approaches resulted in 1.8 to 5.5-fold increase in the rat lung localization ratio for MoAb 9B9 due to the enhancement of the antibody blood clearance.

The pharmacokinetics of ^{111}In-MoAb 9B9 biodistribution in rat is similar to that of ^{125}I-MoAb 9B9 (see Fig. 3, Table 2, (1)). However, there are differences in the kinetics of lung accumulation of MoAb 9B9 radiolabeled with these isotopes: ^{125}I-MoAb 9B9 is retained in the lung for a longer period than ^{111}In-MoAb 9B9. At periods longer than 24 hr postinjection ^{111}In/^{125}I radioactivity ratio in blood increases (see Table 2). This ratio represents the difference in the pharmacokinetics of the corresponding isotopes and/or modified antibodies (*19*).

The observed results may be due to either the rapid dehalogenation or clearance of ^{125}I-MoAb 9B9 from the blood, since ^{111}In and ^{125}I were radiolabeled on different aliquots of 9B9. Khaw et al. dual-labeled the same aliquot MoAb 103D2 against tumor-associated 126 kD phosphoglycoprotein with ^{111}In and ^{125}I and observed that ^{111}In/^{125}I radioactivity ratio remained unchanged for up to 6 days (*19*).

The data presented in Figure 4 and Figure 5 show that ^{111}In-MoAb selectively accumulates in the monkey lung after intravenous injection. This preferential lung uptake is clearly seen in the gamma scintigrams.

It is important to note the differences in biodistribution patterns of [^{111}In]MoAb 9B9 and [^{99m}Tc]albumin microspheres (Fig. 6). The latter is routinely used for perfusion studies in the lung (*20*). Indium-111 MoAb 9B9, on the other hand, may find an application for

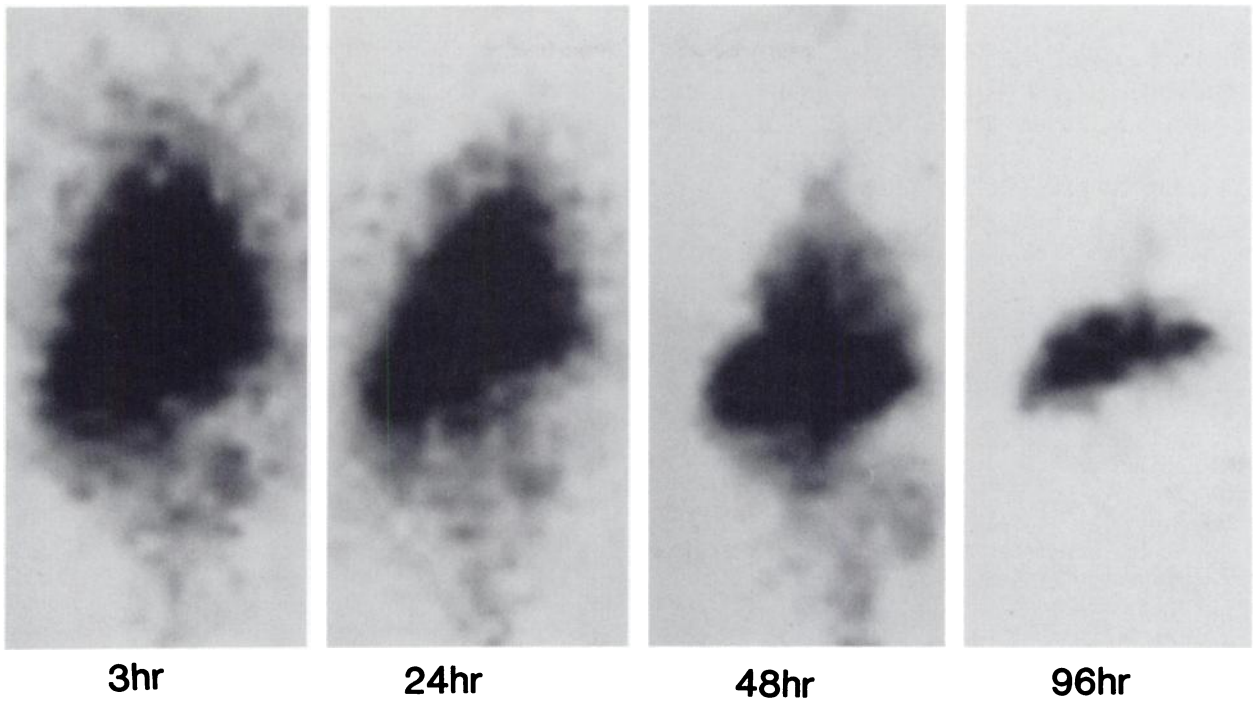

FIGURE 5
Serial anterior thoraco-abdominal images after i.v. injections of ^{111}In-labeled MoAb 9B9 (200 μg, 0.5 mCi) in monkey. Background radioactivity was subtracted from each image. (Correction for radioisotope decay was made).

monitoring the status of the lung endothelium by gamma-scintigraphy. This information is not available by the standard approach with ^{99m}Tc microspheres which measures the characteristics of blood flow only. This is especially important, because the biodistribution pattern of ^{111}In-MoAb 9B9 may change during certain pathological processes in the lung. For instance, lung uptake may be decreased in the case of extensive damage of lung endothelium during adult respiratory distress syndrome (ARDS) (*21*) or in acute pulmonary insult (*22*).

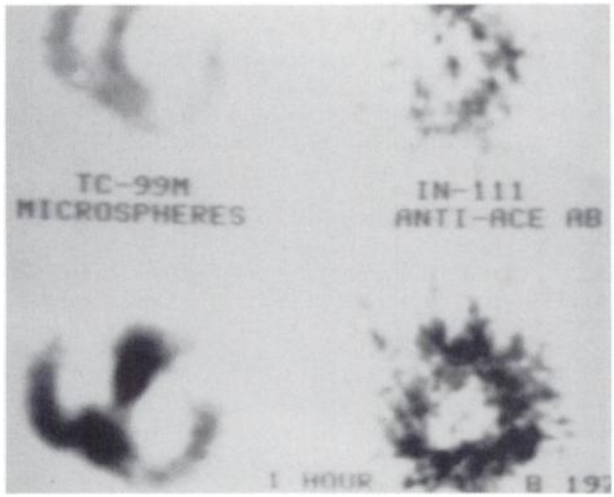

FIGURE 6
Lung accumulation images of ^{111}In-labeled MoAb 9B9 (200 μg, 0.5 mCi) (right) and ^{99m}Tc-labeled albumin microaggregates (0.5 mCi) (left), represented as two tomographic slices, obtained on the same level 1 hr after i.v. injection of these radiolabels in monkey.

It has not yet been proven that 9B9 antibodies will be an adequate tool for such a problem. Still, recent data show that 9B9 MoAb lung accumulation is drastically lowered in the models of rat lung injuries, e.g., α-naphtylthiourea (*23*) or endotoxin (*24*) preinjection (Muzykantov et al: unpublished data). 9B9 MoAb localization ratio in these cases is lowered by 40% to 50%. One can assume from these data that binding of 9B9 antibodies is decreased in case of endothelium injury. It has yet to be shown that these decreases of the lung accumulation are sufficient for the marked changes of corresponding scintigrams.

Furthermore, radiolabeled MoAb 9B9 may find an application in the diagnosis of sarcoidosis. In this disease, granulomas appear in the lung and other tissues, epitheloid and giant cells all of which produce extremely large quantities of ACE (*8*). One can assume that anti-ACE MoAb uptake in the tissues of patients with sarcoidosis should be higher than the corresponding MoAb uptake in healthy individuals. These antibodies may be retained in patients' lung for longer periods of time due to high antigen content in the lung tissues. A similar approach is now widely used for tumor imaging with

radiolabeled antibodies against tumor-specific antigens (*25, 26*).

It may also be possible to use this radiolabeled MoAb 9B9 for the differential diagnosis of lymphangioma and hemangioma as Anti-ACE antibodies injected intravenously should localize in hemangiomas, but not in the lymphangiomas.

Further evaluations of the potential of ^{111}In-labeled monoclonal antibody (9B9) against angiotensin-converting enzyme in clinical studies are planned.

ACKNOWLEDGMENT

The authors thank I. Kharlamov for the photographs.

REFERENCES

1. Danilov SM, Muzykantov VR, Martynov AV, et al. Specific accumulation of monoclonal antibodies against angiotensin-converting enzyme in the rat lung. *Dokl Akad Nauk SSSR (Russ)* 1988; 301:1003–1007.
2. Cusman DW, Cheung US. Concentrations of angiotensin-converting enzyme in tissue of the rat. *Biochim Biophys Acta* 1971; 250:261–265.
3. Ryan J, Chung A, Ammons M, et al. A simple radioassay for angiotensin-converting enzyme. *Biochem J* 1977; 167:501–504.
4. Fishman A. Dynamics of the pulmonary circulation. In: Hamilton WF, Dow P, eds. *Handbook of Physiology, Washington DC. Am Physiol Soc* 1963; 2:1667.
5. Ryan JW, Ryan US, Schultz DR, et al. Subcellular localization of pulmonary angiotensin-converting enzyme (Kininase II). *Biochem J* 1975; 146:497–499.
6. Caldwell PRB, Seegal B, Hsu K, et al. Angiotensin-converting enzyme: vascular endothelial localization. *Science* 1976; 191:1050–1051.
7. Danilov SM, Faerman AI, Printseva OYu, et al. Immunohistochemical study of angiotensin-converting enzyme in human tissues using monoclonal antibodies. *Histochemistry* 1987; 87:487–490.
8. Silverstein E, Pertschuk L, Friedland J. Immunofluorescent localization of angiotensin-converting enzyme in epitheloid and giant cells of sarcoidosis granulomas. *Proc Natl Acad Sci USA* 1979; 76:6646–6648.
9. Danilov SM, Allikmets EY, Sakharov IY, et al. Monoclonal antibody to human lung angiotensin-converting enzyme. *Biotechnol Appl Biochem* 1987; 9:319–322.
10. Fraker PJ, Speck JC. Protein and cell membrane iodinations with a sparingly soluble chloroamide, 1,3,4,6-tetrachloro-3a, 6a-diphenylglycoluril. *Biochem Biophys Res Commun* 1978; 80:849–857.
11. Cole WS, De Nardo SJ, Meares CF, et al. Comparative serum stability of radiochelates for antibody pharmaceuticals. *J Nucl Med* 1987; 28:83–90.
12. Rokhlin OV, Petrosyan MN, Ibragimov AR, et al. Antigenic markers of V domain of mouse MOPS-21 IgG_1 L chain. *Eur J Immunol* 1983; 13:397–403.
13. Sakharov I, Danilov S, Dukhanina E. Affinity chromatography and some properties of the angiotensin-converting enzyme from human heart. *Biochim Biophys Acta* 1987; 923:143–149.
14. Keenan AM, Narbert JC, Larson SM. Monoclonal antibodies in nuclear medicine. *J Nucl Med* 1985; 26:531–537.
15. Rockoff SD, Goodenough DJ, McIntire KR. Theoretical limitations in the immunodiagnostic imaging of cancer with computed tomography and nuclear scanning. *Cancer Res* 1980; 40:3054–3058.
16. Sakahara H, Endo K, Nakashima T, et al. Localization of human osteogenic sarcoma xenograft in nude mice by monoclonal antibody labeled with radioiodine and indium-111. *J Nucl Med* 1987; 28:342–348.
17. Wahl RI, Parker CW, Philiport GW. Improved radioimmunoimaging and localization with monoclonal $F(ab')_2$. *J Nucl Med* 1983; 24:316–325.
18. Klibanov AL, Martynov AV, Slinkin MA, et al. Blood clearance of radiolabeled antibody: enhancement by lactosamination, treatment by biotin-avidin or anti-mouse IgG antibodies. *J Nucl Med* 1988; 29:1951–1956.
19. Khaw BA, Cooney J, Edgington T, et al. Differences in experimental tumor localization of dual labeled monoclonal antibody. *J Nucl Med* 1986; 27:1293–1299.
20. Frankel N, Coleman RE, Pryor DB, et al. Utilizations of lung scan by clinicians. *J Nucl Med* 1986; 27:366–369.
21. Hyers TM, Fowler AA. Adult respiratory distress syndrome: causes, morbidity and mortality. *Fed Proc* 1986; 45:25–29.
22. Hollinger MA, Giri SN, Patwell S, et al. Effect of acute lung injury on angiotensin-converting enzyme in serum, lung lavage and effusate. *Am Rev Resp Dis* 1980; 121:373–376.
23. Martin D, Korthnis RJ, Perry M, et al. Oxygen mediated lung damage associated with naphtylthiourea. *Acta Physiol Scand Suppl* 1986; 548:119–125.
24. Meyrick BO. Endotoxin-mediated pulmonary endothelial cell injury. *Fed Proc* 1986; 45:19–24.
25. Chatal JF, Thedpez P, Blottiere H, et al. Comparative characteristics of 17-1A and GA-733 monoclonal antibodies for immunoscintigraphic application. *Hybridoma* 1986; 5 (suppl 1):587–596.
26. Larson SM. Radiolabeled monoclonal antitumor antibodies in diagnosis and therapy. *J Nucl Med* 1985; 26:538–545.